

INFLUENCE OF INTERFACIAL VOID AROUND REINFORCEMENT DUE TO BLEEDING ON CHLORIDE INGRESS AND ITS INTERACTION WITH FLEXURAL CRACK

Nguyen Thi Hien^{*1}, Ryohei Ohara^{*1}, Takumi Shimomura^{*2}

ABSTRACT

Chloride-induced reinforcement corrosion in reinforced concrete structures exposing marine environment is one of the most importance factors affecting the durability of structures. In this paper, the influence of interfacial void around reinforcement due to bleeding on chloride ingress in RC members with flexural cracks is investigated through experiment and numerical simulation. The influence of interfacial void and its interaction between flexural cracks on chloride ingress into concrete under various conditions are systematically investigated through numerical simulation.

Keywords: chloride ingress, bleeding, interfacial void, flexural crack, crack width.

1. INTRODUCTION

The main cause of deterioration of reinforced concrete structures is corrosion of embedded reinforcing steel bar due to chloride, in particular, under marine environments or deicing salts. In the Standard Specification for Concrete Structures by Japanese Society of Civil Engineers (JSCE), the effect of flexural crack width and quality of concrete are synthetically taken into account in calculating chloride ion concentration at the location of reinforcing bar since 2002. Based on this framework, many studies have been done to enhance evaluation of durability of RC structures in terms of prediction of the migration of chlorides into concrete.

Flexural cracks are generally allowed in RC member under service load by restricting crack width as small as harmless width. On the other hand, the influence of damage of the steel-concrete interface due to increased tensile stress or cyclic load on chloride ingress has been confirmed in a few studies [1] [2]. It was found that the damage of steel- concrete interface was an important factor in chloride ingress and subsequent reinforcement corrosion. Damage of steel-concrete interface is caused also by concrete bleeding resulting in the formation of interfacial void around reinforcing bar.

In this study, the influence of interfacial void around reinforcement due to bleeding on chloride ingress in RC members is investigated through experiment and numerical simulation. The influence of interfacial void and its interaction between flexural cracks on chloride ingress into concrete under various conditions are systematically investigated through numerical simulation, in which transport of water and chloride through flexural crack and interfacial void are considered.

2. EXPERIMENTAL INVESTIGATION

2.1 Specimen

Reinforced concrete specimens, whose sizes are 100mm x 100mm x 800 mm and 100mm x 500mm x 800 mm, were prepared as shown in Fig. 1. One deformed steel bar of 13mm in diameter was embedded in the longitudinal direction in the specimens, with 50mm concrete cover from the top surface. The big specimen with 500mm depth was intended to generate greater bleeding than the small specimen with 100mm depth. Table 1 shows the mix proportion of concrete used. To ensure much bleeding, unit water was set as 175 kg/mm³.

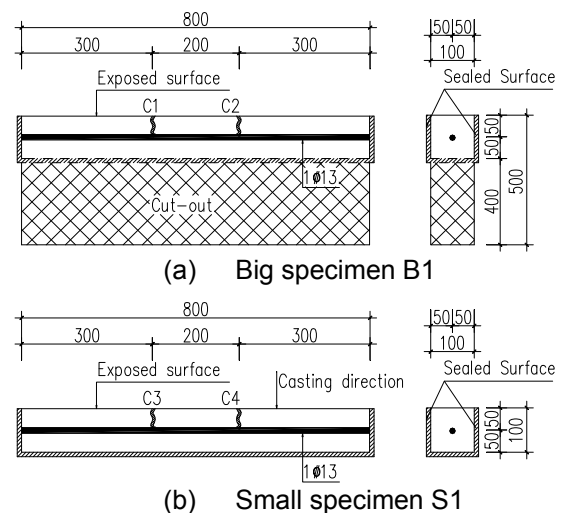


Fig.1 Layout of specimen

Table 1 Concrete mix proportion

W/C (%)	s/a (%)	Kg/m ³			
		W	C	S	G
60	45	175	292	793	1006

*1 Graduate School of Engineering, Nagaoka University of Technology, JCI Student Member

*2 Prof., Dept. of Civil and Environmental Engineering, Nagaoka University of Technology, Dr.E., JCI Member

Table 2 Detail of specimens

No.	Size (mm)	c (mm)	Crack width (mm)	Crack interval (mm)
B1	500x100x800	45	0.135 (C1) 0.037 (C2)	200
S1	100x100x800		0.037 (C3) 0 (C4)	

After curing by wrapping with wet mattress for 28 days in the laboratory, lower part of the big specimen was cut out by a cutting machine as shown in Fig. 1a. Then, slits with 3mm depth and 5mm width were induced in the specimens using a cutting machine to initiate flexural cracks at the designated position. Flexural cracks were induced by four-point-loading. Cracks are named as C1, C2, C3 and C4 as shown in Fig.1. The widths of the cracks are presented in Table 2, which were measured by π gauge and controlled by inserting aluminum plates into the slits. In order to control the penetration of chloride ions into concrete, all surfaces except the exposed surface of the specimens were sealed with epoxy-type adhesive. Then, all specimens were placed in a chamber with constant temperature and humidity and periodical drying-wetting actions using a sodium chloride solution (5% NaCl). The length of one cycle was set 1 day consisting of 12 hours (1/2 day) mist containing 5% sodium chloride solution at 40°C temperature and 100% relative humidity and 12 hours (1/2 day) drying at 40°C temperature and 60% relative humidity.

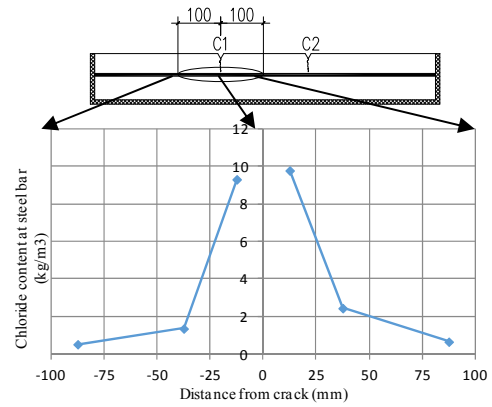
After 38 days exposure test, specimens were taken out from the chamber and samples of concrete powder were taken from around the steel bar in the specimens using an electric drill. Chloride content in concrete was measured with a chloride ion meter.

2.2 Test Results

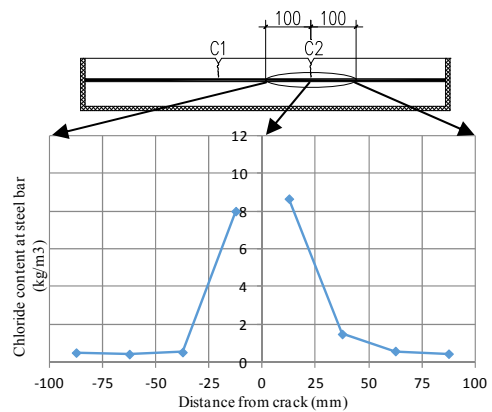
Fig. 2 shows the experimental results of chloride content in concrete along reinforcing bar in the specimens after 38 days exposure test. Firstly, it is regarded in both specimens that chloride content along reinforcing bar descends in accordance with the distance from crack.

Secondly, chloride content around crack C2 in specimen B1 is greater than crack C3 in specimen S1 even though the crack width of both cracks is same as 0.037mm. It is attributable to the existence of interfacial void around reinforcing, whose photographs are shown in Fig. 3. Bleeding in specimen B1 was obviously more than in specimen S1. It is clear in Fig. 3 that interfacial void around reinforcing bar in specimen B1 is greater than in specimen S1.

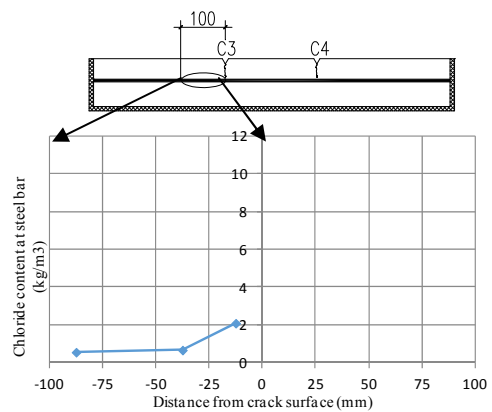
Thirdly, comparing crack C1 and C2 in specimen B1, chloride content around C1 whose width is 0.135mm is more than around C2 whose width is 0.037mm. This suggests that chloride ingress into concrete from crack surface is promoted with increasing of crack width.



C1 in Specimen B1 (w=0.135mm)



C2 in Specimen B1 (w=0.037mm)



C3 in Specimen S1 (w=0.037mm)

Fig. 2 Experimental results of chloride content along reinforcing bar after 38 days of exposure



(a).Specimen B1 (b).Specimen S1

Fig. 3 Interfacial void around reinforcement

3. METHOD OF NUMERICAL SIMULATION

Numerical simulation of transport of water and chloride was carried out to verify the influence of interfacial void around reinforcement on chloride ingress into RC members and its interaction with cracks. The layout of a part of RC member with flexural crack and bleeding void is shown in Fig. 4, in which L is crack interval, w is crack width, v_w is width of interfacial void, c is thickness of concrete cover. Water and chloride ions are assumed to penetrate into concrete from the exposed surface, the crack surface and the surface of interfacial void around reinforcement.

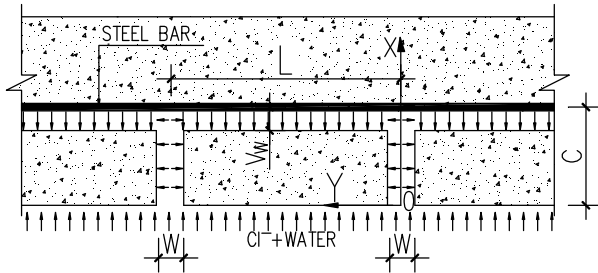


Fig. 4 Layout of RC member with flexural crack and interfacial void

3.1 Penetration of Liquid Water into Concrete within Crack and Interfacial Void [3]

The max flux of liquid water by capillary suction in concrete is evaluated as follows:

$$J_{lp} = \int_{r_a}^{\infty} \rho_l \frac{dV_{(r)}}{dr} \left\{ K_{lp} \sqrt{\frac{r\gamma}{8\mu t_{cap}}} \right\} dr \quad (1)$$

where $V_{(r)}$ is pore size distribution function [m^3/m^3], μ is viscosity of liquid water [$Pa*s$], K_{lp} is non-dimensional frictional coefficient, r_a is threshold pore radius (m), t_{cap} is time from the beginning of wetting process (sec)

The mass flux of capillary suction water in crack (J_{lp}^{cr}) and interfacial void (J_{lp}^{iv}) are evaluated, respectively, as:

$$J_{lp}^{cr} = \rho_l \sqrt{\frac{w\gamma}{2ft}} \quad (2)$$

$$J_{lp}^{iv} = \rho_l \sqrt{\frac{v_w\gamma}{2ft}} \quad (3)$$

where γ is surface tension of water (N/m) and f is friction factor for transport of liquid water within crack and interfacial void ($kg/m.s$), ρ_l is density of liquid water (kg/m^3), t is time from the initiation of wetting process (sec). The value of f is determined based on sensitivity analysis in Chapter 5.

When concrete surface directly contacts with liquid water, liquid water penetrates into crack and interfacial void around reinforcement by capillary suction. Thereafter, liquid water ingresses into concrete from three surfaces: the exposed surface, the crack surface and the surface of interfacial void around

reinforcement. The amount of penetrated water into concrete from the crack surface and the surface of interfacial void around reinforcement does not exceed the amount of water in the crack and the void respectively. When all liquid water in crack and void has penetrated into concrete, liquid water penetrates into concrete only from the exposed surface as shown in Fig. 5.

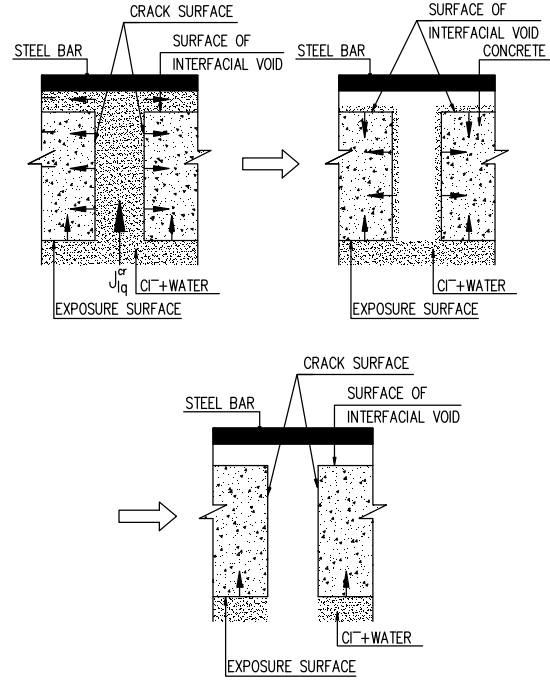


Fig. 5 Penetration of liquid water into crack and interfacial void around reinforcement

3.2 Drying from the Crack Surface and the Surface of the Interfacial Void

The evaporation of water from concrete surface is evaluated by the following equation:

$$J_B = \frac{D(w_l)}{h} (w_l - w_{lB}) \quad (4)$$

where J_B is mass flux of water through the boundary surface [$kg/m^2/s$], w_l is water content of concrete at the surface [kg/m^3], w_{lB} is water content in equilibrium with atmosphere [kg/m^3], $D(w_l)$ is equivalent moisture diffusivity at the boundary [m^2/s], h is thickness of boundary film representing the state of humidity distribution in the atmosphere near the surface, which is 0.00075(m) at the ordinarily exposed surface.

The evaporation of water from crack surface and surface of interfacial void are evaluated, respectively, as:

$$J_{Bcr} = \beta_{cr} J_B \quad (5)$$

$$J_{Bv} = \beta_v J_B \quad (6)$$

where J_{Bcr} is mass flux of water through the boundary surface of crack [$kg/m^2/s$], J_{Bv} is mass flux of water

through the boundary surface of interfacial void [kg/m²/s], β_{cr} is non-dimensional factor which represents reduction ratio of evaporation from crack surface, β_v is non-dimensional factor which represents reduction ratio of evaporation from surface of interfacial void. In this study, the value of β_{cr} and β_v are determined based on sensitivity analysis in Chapter 5.

3.3 Transport of Chloride Ions

Transport of chloride ions in concrete is calculated with considering molecular diffusion of free chloride ions within liquid water and mass flux of free chloride ions carried by liquid water:

$$\frac{\partial C_{Clt}}{\partial t} = -\text{div} \left(J_{Cl dif} + C_{freeCl} \frac{J_{lp}}{\rho_l} \right) \quad (7)$$

where C_{Clt} is total mass concentration of chloride per unit concrete volume, $J_{Cl dif}$ is mass flux of chloride by diffusion, J_{lp} is mass flux of liquid water, C_{freeCl} is mass concentration of free chloride.

The max flux of chloride ions by diffusion is calculated as:

$$J_{Cl dif} = -K_{Cl} D_{Cl} \text{grad} C_{freeCl} \quad (8)$$

where K_{Cl} is non-dimensional material factor which presents the effect of narrowness and tortuosity of the pore structures of concrete, D_{Cl} is diffusivity of chloride ion in liquid water.

In this study, capillary suction from concrete surface is considered as transport mechanism of liquid water.

The transition between free and fixed chloride is calculated based on the equation proposed by Maruya et.al [3]:

$$C_{Clf} = \alpha C_{Clt} \quad (9)$$

where α is fixing rate of chloride ions with cement hydrate in hardened concrete formulated as a function of C_{Clt} and the type of cement.

4. SIMULATION OF EXPERIMENTAL RESULTS

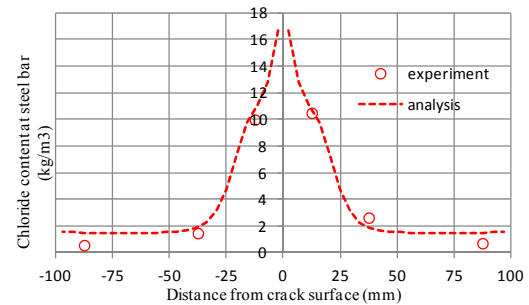
Non-dimensional factor for evaporation from the crack surface (β_{cr}) and the surface of interfacial void (β_v) are determined so that the experimental results of three cases could be appropriately simulated by the computational model based on the sensitivity analysis that will be shown in Chapter 5. The determined parameters are listed in Table 3. These parameters are commonly used in the three cases

Table 3 Material parameters

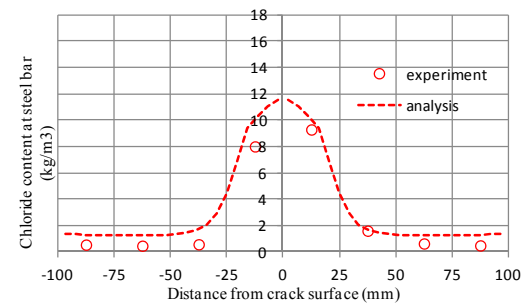
β_v	β_{cr} (w=0.135mm)	β_{cr} (w=0.037mm)
1.0	1.0	0.01

The width of the void at steel-concrete interface in specimen B1 was assumed 0.01mm according to the measurement results by microscope, while no interfacial void was provided in specimen S1. Fig. 6

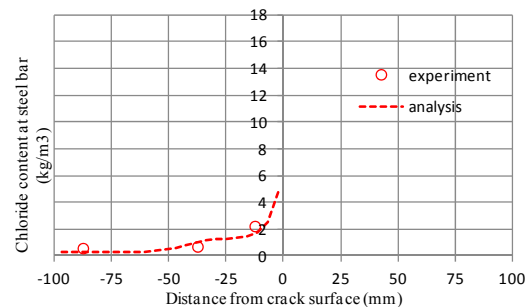
shows the comparison of experimental chloride distribution and analytical ones along reinforcement in concrete. The tendency of chloride distribution around cracks: C1, C2 and C3 are all well simulated by the analysis. The analysis can adequately express the influence of crack and interfacial void around reinforcement observed in the experiment.



C1 in Specimen B1 (w=0.135mm)



C2 in Specimen B1 (w=0.037mm)



C3 in Specimen S1 (w=0.037mm)

Fig. 6 Comparison of experimental and analytical chloride content along reinforcing bar after 38 days of exposure

5. SENSITIVITY ANALYSIS OF THE EFFECT OF INTERFACIAL VOID ON CHLORIDE INGRESS

5.1 Analytical Cases

In order to investigate the sensitivity of the effect of the interfacial void around reinforcement induced by bleeding on chloride ingress and its interaction with flexural crack, systematic numerical experiment of unknown parameters was carried out. Table 4 shows experimental parameters and their variation examined. 10 cases shown in Table 5 are calculated in total.

Table 4 Experimental parameters and their variation

Experimental parameters	Variations
Void width (v_w) (mm)	0.01, 0.05, 0.1
Friction factor (f) (kg/m.s)	0.02, 20, 2000
Non-dimension factor for evaporation rate from crack surface (β_{cr})	1.0, 0.1, 0.01
Non-dimension factor for evaporation rate from surface of interfacial void (β_v)	1.0, 0.1, 0.01

Table 5 Calculated cases in parametric study

Case	v_w (mm)	f (kg/m.s)	β_{cr}	β_v	L (mm)
1	0.01	20	1	1	200
2	0.1	20	1	1	
3	0.5	20	1	1	
4	0.01	0.02	1	1	
5	0.01	200	1	1	
6	0.01	20	1	0.1	
7	0.01	20	1	0.01	
8	0	20	1	1	
9	0	20	0.1	1	
10	0	20	0.01	1	

5.2 Results and Discussion

Calculated chloride content at the location of reinforcing steel bar as a function of distance from crack after 38days' exposure is presented in Fig. 7 to Fig. 10.

(1) Influence of void width

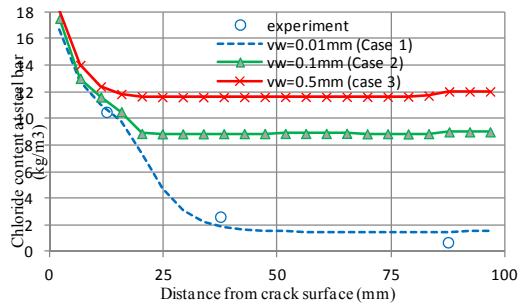


Fig. 7 Chloride content along reinforcing bar in concrete with various width of interfacial void ($w=0.135\text{mm}$)

Fig. 7 shows the influence of void width on chloride content at the position of reinforcing bar. Three widths of interfacial void are examined: 0.01mm, 0.1mm and 0.5mm. The crack width is set as 0.135mm. It can be seen that chloride content along reinforcing bar increases with increasing of void width. This suggests that crack width control is effective when defect due to bleeding around reinforcement does not exist. In addition, it is confirmed that analytical results correspond with experimental results when void width is assumed 0.01mm.

(2) Influence of friction factor

The influence of friction factor for transport of liquid water within crack and interfacial void on

chloride content at the position of reinforcing bar is shown in Fig. 8. Three values of friction factor are examined: 0.02 kg/m.s, 20 kg/m.s and 200 kg/m.s. The width of crack is 0.135mm in the series. According to the results, chloride content at the location of steel bar increases with decreasing of friction factor. In addition, analytical result agrees well with experimental result when friction factor is 20kg/m.s.

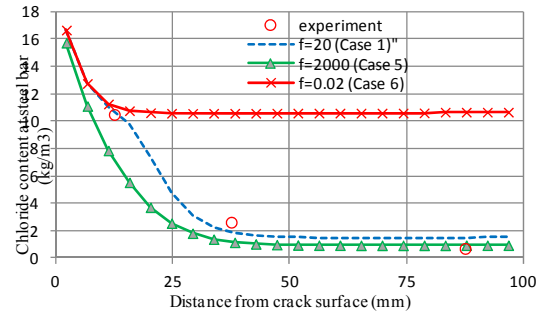


Fig. 8 Chloride content along reinforcing bar in concrete with various value of friction factor ($w=0.135\text{mm}$, $v_w=0.01\text{mm}$)

(3) Influence of β_v

Fig. 9 shows the influence of non-dimension factor for evaporation from the surface of interfacial void on chloride content at the position of reinforcing bar. Three values of β_v are examined: 1.0, 0.1 and 0.01. Crack width is 0.135mm and the width of interfacial void is assumed 0.01mm. It is clear that chloride content at the location of reinforcing bar increases with increasing of β_v . According to the results, analytical results agree well experimental results when value of β_v is 1.

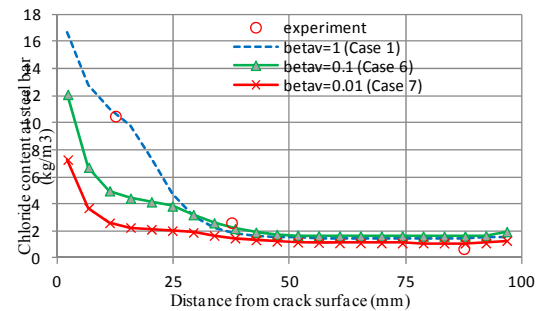


Fig. 9 Chloride content along of reinforcing bar in concrete with various value of β_v ($w=0.135\text{mm}$, $v_w=0.01\text{mm}$)

(4) Influence of β_{cr}

Fig. 10 shows the influence of non-dimension factor for evaporation from the surface of interfacial void on chloride content at the position of reinforcing bar. Three values of β_{cr} are examined: 1.0, 0.1 and 0.01. Crack width is 0.037mm and no interfacial void is provided around reinforcement. According to the results, chloride content at the location of reinforcement increases with increasing of β_{cr} . This suggests that evaporation from crack surface is reduced when crack width is small. Analytical results agree well

experimental results when value of β_{cr} is 0.01.

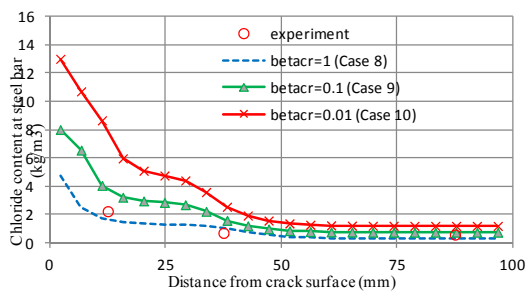


Fig. 10 Chloride content along of reinforcing bar in concrete with various thickness of β_{cr} ($w=0.037\text{mm}$, $vw=0$)

5. CONCLUSION

Followings conclusions can be drawn from the conducted experiment and analysis:

- (1) It was experimentally confirmed that the interfacial void around reinforcement due to bleeding accelerates transport of chloride ions in RC member.
- (2) Experimental results of chloride ingress into RC member can be simulated by numerical analysis in which transport of water and chloride through flexural crack and the interfacial void around reinforcement are considered.
- (3) The results of conducted parametric sensitivity analysis suggested that defect around reinforcement due to bleeding should be avoided to make crack width control in RC member effective.
- (4) Chloride ingress into concrete with flexural crack and interfacial void around reinforcement due to bleeding could be simulated by numerical analysis using parameters which were determined based on the parametric analysis.

ACKNOWLEDGEMENT

This work was supported by JSPS Grants-in-Aid for Scientific Research, Grant Number 25289131.

REFERENCES

- [1] Savija, B., Schlangen, E., Pacheco, J., Millar, S., Eichler, T., & Wilsch, G., "Chloride ingress in cracked concrete: a laser induced breakdown spectroscopy (LIBS) study", *Journal of Advanced Concrete Technology*, Vol. 12, No. 10, pp. 425-442, 2014
- [2] Pease, Bradley Justin; Geiker, Mette Rica; Stang, Henrik; Weiss, Jason, "Photogrammetric assessment of flexure induced cracking of reinforced concrete beams under service loads", 2nd International RILEM Symposium, 2006
- [3] S. Kobayashi and T. Shimomura, "Numerical Analysis on Transport of Aggressive Materials and Corrosion of Steel Bars in Concrete," *Proceedings of the Japan Concrete Institute*, Vol. 24, No. 1, pp. 831-836, 2002
- [4] Goto, Y., "Cracks formed in concrete around deformed tension bars", *ACI Journal*, Vol. 68, No. 4, pp. 35-47, 1970
- [5] T. Shimomura and K. Maekawa., "Analysis of the drying shrinkage behavior of concrete using a micromechanical model based on the microspore structure of concrete," *Magazine of Concrete Research*, Vol. 49, No. 181, pp. 303-322, 1977
- [6] Maruya, T., Somnuk, T. and Matsuoka, Y. "Simulation of chloride penetration into hardened concrete," *Proceedings of the CANMET/ACI International Conference of Durability of Concrete*, pp. 519-538, 1994
- [7] H. Thynn Thynn and T. Shimomura., "Hybrid computational method for capillary suction and nonsaturated diffusion in concrete", 4th International Conference on Construction Materials ConMat'09, pp. 1075-1080, 2009
- [8] JSCE., "Standard Specification for Concrete Structures-2012 Design", *Japan Society of Civil Engineers*, 2012